



Received 12 June 2024, accepted 15 July 2024, date of publication 19 July 2024, date of current version 19 August 2024.

Digital Object Identifier 10.1109/ACCESS.2024.3431026

## RESEARCH ARTICLE

# Design and Test of High-Low Voltage Excitation System for HTS Synchronous Condenser

JINFENG WANG<sup>1</sup>, Tiantian CAO<sup>1</sup><sup>2</sup>, YUFENG DAI<sup>2</sup>, SIQI XIE<sup>2</sup>, ZHU LIU<sup>3</sup>,  
AND DAYI LI<sup>1</sup><sup>2</sup>, (Member, IEEE)

<sup>1</sup>Electric Power Science Research Institute of Guangdong Electric Power Company Ltd., Guangzhou 510000, China

<sup>2</sup>School of Electrical and Electronic Engineering, Huazhong University of Science and Technology, Wuhan 430074, China

<sup>3</sup>China Southern Power Grid Research Technology Co., Ltd., Guangzhou 510000, China

Corresponding author: Dayi Li (ldy@mail.hust.edu.cn)

This work was supported by the Science and Technology Project of China Southern Power Grid Company Ltd., under Grant GDKJXM20222474.


**ABSTRACT** Temperature superconducting (HTS) synchronous condenser is a reactive power compensation device with the advantages of low loss, high efficiency and wide reactive power range. Therefore, it has a very good application prospect in power grid. To solve the problems of low power factor and low conduction angle of constant excitation function for a long time due to single power supply excitation system, this paper proposes a high-low voltage switching excitation system, which separates the forced excitation and constant excitation modes of the excitation system into two power supplies. Based on the introduction of principle of excitation system, the design of its parameters and simulation analysis are completed, and a set of 400kW device is designed. On this basis, a series of corresponding superconducting experiment are carried out. The experimental results verify the principle of the power supply topology, and also show the feasibility and reliability of the proposed excitation system.

**INDEX TERMS** HTS synchronous condenser, high and low voltage switching, excitation system, superconducting experiment.

## I. INTRODUCTION

With the development of ultra-high voltage direct current transmission circuit in the power grid, the emergence of various new energy power generation devices, and the use of various flexible power electronics, the imbalance between active power and reactive power in the power grid is becoming more and more serious [1], [2].

The high temperature superconducting (HTS) synchronous condenser with the rotor made of superconducting materials is a combination of high-capacity synchronous condenser and superconducting technology [3], [4], [5]. It has lots of advantages compared with traditional reactive power compensation device, such as low loss, small size, wide reactive power range and so on. Its performance of reactive power compensation is better than conventional synchronous condenser [6], [7], [8].

The associate editor coordinating the review of this manuscript and approving it for publication was Alon Kuperman<sup>1</sup>.

Most of the time, the exciting current of HTS synchronous condenser is stable, which is called constant excitation mode. When the exciting current need to be increased quickly in a short time, this mode is called forced excitation mode.

The excitation system of conventional synchronous condenser always uses single power supply, which provides power to constant excitation mode and forced excitation mode at the same time. Consequently, it will lead to a series of problems such as low power factor of excitation transformer, serious distortion of current waveform at AC side. For the HTS synchronous condenser, its rotor is equivalent to a large inductance, which requires a larger forced excitation multiple of the excitation power supply [9], [10]. Therefore, the conventional excitation system is not suitable for HTS synchronous condenser.

The research content of this paper is to design an excitation system for the 10Mvar HTS synchronous condenser that being developed by China Southern Power Grid Corporation.

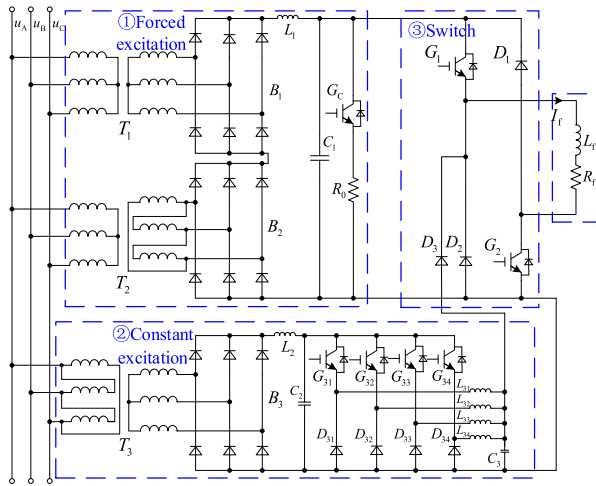


FIGURE 1. High-low voltage switching dual power supply topology.

To solve these problems, a high-low voltage switching excitation system is proposed in this paper, which can separate forced excitation mode and constant excitation mode. The simulation and experimental results show the feasibility of the proposed excitation system. Compared with the conventional excitation system, it has certain application advantages.

II. PRINCIPLE ANALYSIS AND PARAMETER DESIGN

In this paper, a high-low voltage switching dual power supply topology is proposed, as shown in Fig. 1. Since the working voltage of constant excitation mode is much lower than that of forced excitation mode, the corresponding voltages are called low voltage and high voltage respectively.

It is reported that the excitation inductance of a 10Mvar HTS synchronous condenser is about 5.86H [9]. To highlight the main characteristic and simplify the analysis, the HTS excitation winding is equvalued as a series connection of inductance  $L_f$  and resistance  $R_f$ . Therein,  $R_f$  is the total resistance of the excitation system,  $L_f$  is the inductance of the HTS rotor. This excitation system adopts dynamic current closed-loop control strategy, it also has the function of forced excitation and quick deexcitation, thus the inductance nonlinearity of the HTS excitation winding will have little impact on the stability of excitation current.

A. EQUATIONS

The high voltage module required by forced excitation mode is composed of 12-pulse rectifier transformer T1 and T2 and uncontrolled rectifier bridge B1 and B2. Then a filter circuit which is formed by L1 and C1 is followed. Meanwhile, the capacitor C1 can be used to store the energy required by forced excitation.

The transformation ratio relationship of 12-pulse rectifier transformer group is designed to be

$$N_{A1} : N_{a1} : N_{A2} : N_{a2} = 1 : n : 1 : \sqrt{3}n \quad (1)$$

where  $N_{A1}$  is the number of turns on primary side of  $T_1$ ,  $N_{a1}$  is the number of turns on secondary side of  $T_1$ . And  $N_{A2}$  is

the number of turns on primary side of  $T_2$ ,  $N_{a2}$  is the number of turns on secondary side of  $T_2$ .

The output voltage of the series 12-pulse rectifier bridge is twice that of the 6-pulse rectifier bridge. And the output voltage at the high voltage side can be expressed as

$$U_d = 2 \times 2.34U_2 = 4.68nU_1 \quad (2)$$

where  $U_2$  is the RMS voltage at the secondary side of  $T_1$ ,  $U_d$  is the DC voltage at the high voltage side.

The function of the input filter capacitor C1 is to ensure the voltage stability of the DC bus on the input side. The capacitor will produce voltage ripple  $\Delta V_C$  during charging and discharging. In addition, it should be noted that the series equivalent resistance of capacitor will also produce additional ripple  $\Delta V_{ESR}$ . The total output voltage ripple  $\Delta V$  is given as

$$\Delta V = \Delta V_C + \Delta V_{ESR} \quad (3)$$

$$\Delta V_C = \frac{T_r \Delta I}{4C_1} \quad (4)$$

$$\Delta V_{ESR} = R_{ESR} \Delta I \quad (5)$$

where  $T_r$  is the current ripple period,  $\Delta I$  is the current ripple magnitude through the capacitor, and  $R_{ESR}$  is the equivalent series resistance of the capacitor. From (3) to (5), the expression of capacitance  $C_1$  can be deduced as

$$C_1 = \frac{T_r \Delta I}{4(\Delta V - R_{ESR} \Delta I)} \quad (6)$$

The function of inductor  $L_1$  is to smooth the current input to the next stage. The cut-off frequency  $f_{ci}$  of the input filter circuit, which is expressed as

$$f_{ci} = \frac{1}{2\pi \sqrt{L_1 C_1}} \quad (7)$$

can be taken as 1/10 of the switching frequency. Combined with (6) and (7), it can be obtained that

$$L_1 = \frac{\Delta V - R_{ESR} \Delta I}{\pi^2 f_{ci}^2 T_r \Delta I} \quad (8)$$

B. DESIGN OF CONSTANT EXCITATION MODE

The low voltage module required by the constant excitation mode is composed of 6-pulse rectifier transformer T3 and controllable rectifier bridge B3. Then a four-phase interleaved parallel buck circuit and a filter circuit is followed. Four-phase interleaved parallel buck circuit can reduce the current ripple and improve the effectivity of filtering effect [11], [12]. The transformation ratio relationship of 6-pulse rectifier transformer is

$$N_{11} : N_{12} = 1 : m \quad (9)$$

where  $N_{11}$  is the number of turns on primary side of  $T_3$ , and  $N_{12}$  is the number of turns on secondary side of  $T_3$ . And the output voltage  $U_{d2}$  is

$$U_{d2} = 2.34mU_3 D \cos \alpha \quad (10)$$

where  $\alpha$  is the control angle of bridge  $B_3$ ,  $U_3$  is the RMS voltage at the primary side of  $T_3$ ,  $D$  is the output duty cycle of the interleaved parallel buck circuit.

It is only considered that the circuit works in continuous current mode (CCM), and the current ripple  $\Delta I_L$  of single-phase branch is shown as

$$\Delta I_L = \frac{V_o}{L_f} (1 - D) T_s = \frac{V_{in} D (1 - D) T_s}{L_f} \quad (11)$$

where  $V_o$  is the output voltage of the buck module,  $V_{in}$  is the input voltage of the buck module, and  $T_s$  is the switching cycle of the branch.

For an interleaved parallel buck circuit, the output ripple is related to the duty cycle  $D$  and the number of phases  $N$ . The current fluctuation rate  $r_N$  is defined as the ratio of the peak-to-peak value of current ripple to its DC component  $I_o$ . The current fluctuation rate of single-phase buck converter  $r_1$  is

$$r_1 = \frac{\Delta I_L}{I_o} = \frac{i_{L \max} - i_{L \min}}{I_o} \quad (12)$$

Then, for the  $N$ -phase interleaved buck circuit, the total current fluctuation rate  $r_N$  is

$$r_N = \frac{\Delta I_{LN}}{NI_o} = \frac{i_{LN \max} - i_{LN \min}}{NI_o} \quad (13)$$

The duty cycle  $D$  is divided into  $N$  segments,  $D \in [h/N, (h+1)/N]$ , where  $0 \leq h \leq N-1$ . Then, the falling stage of the total output current is formed by the superposition of  $h$ th single-phase current rising stages with a slope of  $\Delta I_L/DT_s$  and  $(N-h)$ th single-phase current falling stages with a slope of  $\Delta I_L(1-D)T_s$ . Therefore, the total current ripple  $\Delta I_{LN}$  of  $N$ -phase interleaved parallel buck converter is

$$\begin{aligned} \Delta I_{LN} &= \left[ (N-h) \frac{\Delta I_L}{(1-D)T_s} - h \frac{\Delta I_L}{DT_s} \right] \times \left( \frac{T_s(h+1)}{N} - DT_s \right) \\ &= \frac{\Delta I_L (DN - h)(h + 1 - DN)}{DN(1-D)} \end{aligned} \quad (14)$$

Then, the current fluctuation rate  $r_N$  of  $N$ -phase interleaved parallel buck converter can be calculated as

$$r_N = \frac{\Delta I_{LN}}{NI_o} = \frac{(1-ND)\Delta I_L}{NI_o} = \frac{\Delta I_L (DN - h)(h + 1 - DN)}{N^2 I_o D (1-D)} \quad (15)$$

Taking the current fluctuation rate  $r_1$  of the single-phase buck as the benchmark, the ratio  $K_N$  of the  $N$ -phase total output current ripple rate to the single-phase current ripple rate is given by

$$K_N = \frac{r_N}{r_1} = \frac{(DN - h)(h + 1 - DN)}{N^2 D (1-D)} \quad (16)$$

For the four-phase interleaved parallel buck circuit adopted in this paper, the relationship between  $K_N$  and duty cycle  $D$

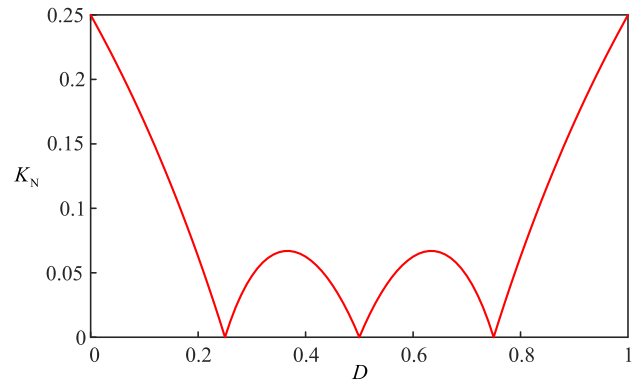


FIGURE 2. The curve of ratio  $K_N$  with duty cycle  $D$ .

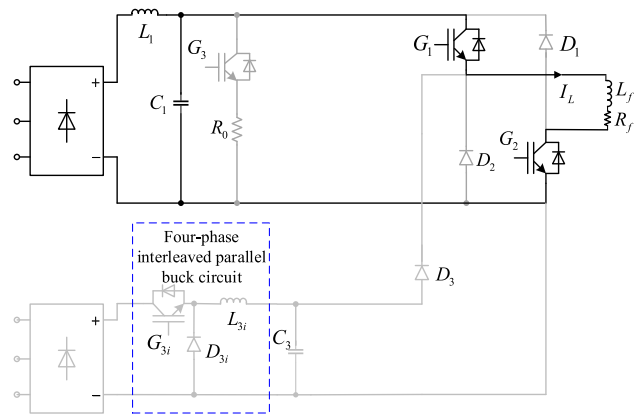


FIGURE 3. Current circuit of forced excitation mode.

can be specified to be

$$K_N = \begin{cases} \frac{1-4D}{4(1-D)}, & D \in \left[0, \frac{1}{4}\right] \\ \frac{(4D-1)(1-2D)}{8D(1-D)}, & D \in \left[\frac{1}{4}, \frac{2}{4}\right] \\ \frac{(2D-1)(3-4D)}{8D(1-D)}, & D \in \left[\frac{2}{4}, \frac{3}{4}\right] \\ \frac{4D-3}{4D}, & D \in \left[\frac{3}{4}, 1\right] \end{cases} \quad (17)$$

According to (17), when  $N = 4$ , the curve of  $K_N$  with duty cycle  $D$  can be illustrated in Fig. 2. It is shown that the total current ripple is 0 theoretically when the duty cycle  $D$  is at 1/4 or 1/2 or 3/4. Consequently, the current ripple can be effectively reduced by making the duty cycle approach these values with some proper control strategies.

### C. ANALYSIS OF CURRENT CIRCUIT IN DIFFERENT WORKING MODES

Different exciting current circuits under various working mode can be realized by the combination of high-voltage power supply, low-voltage power supply and IGBTs. The current circuit under the forced excitation mode is shown as Fig. 3. In this mode, the switches  $G_1$  and  $G_2$  are turned

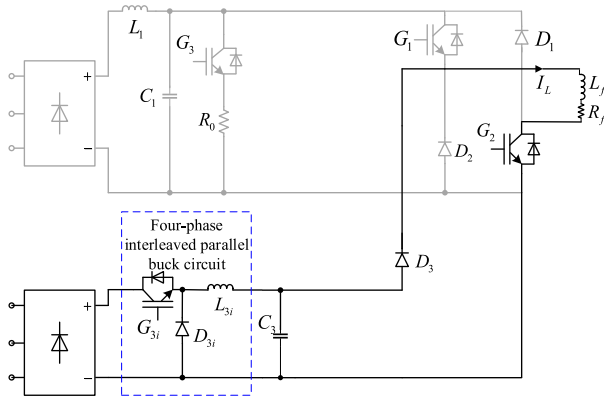


FIGURE 4. Current circuit of constant excitation mode.

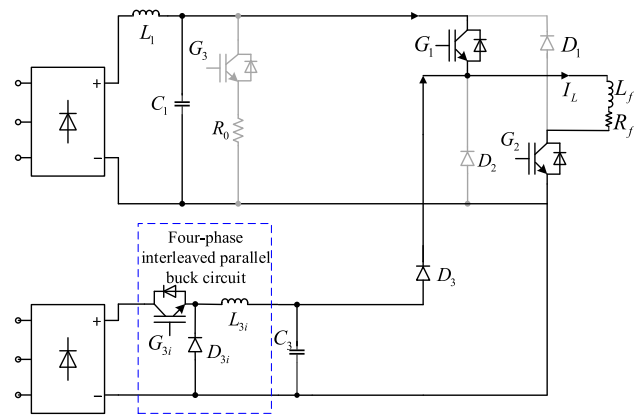


FIGURE 5. Current circuit during switching from constant excitation to forced excitation.

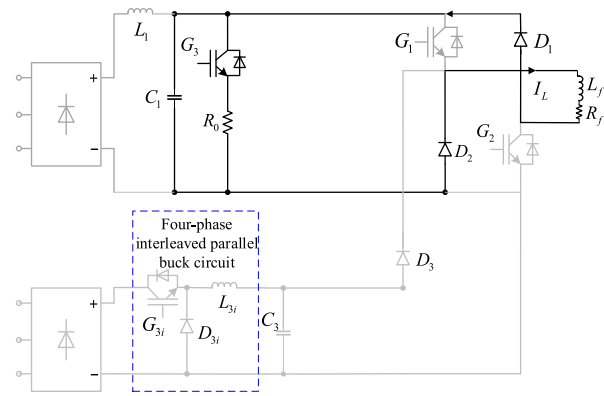


FIGURE 6. Current circuit of de-excitation mode.

on with the high voltage directly applied to the excitation winding, making the exciting current rise rapidly. By this time, D3 is turned off under the reverse voltage, so the low voltage module is unexcited.

Under the constant excitation working mode, the current circuit is depicted in Fig. 4. In this mode, the switches  $G_1$  is turned off and  $G_2$  is turned on, then  $D_3$  can be turned on under the forward voltage, and the four-phase interleaved parallel buck circuit would provide high-precision current for the excitation winding.

TABLE 1. Simulation parameters of excitation system.

Parameter	Value
Forced excitation DC voltage $V_h$	800V
Constant excitation DC voltage $V_l$	48V
Equivalent Inductance $L_f$	5.86H
Total Resistance $R_f$	0.02Ω
Input Capacitance $C_1$	2200uF
Input Inductance $L_1$	0.3mH
Branch Inductance $L_{3i}$	0.05mH
Output Capacitance $C_3$	680uF

TABLE 2. The working value of exciting current.

Working mode	Current/A
Forced excitation	0-300
Constant excitation	300
Forced excitation	300-400
Constant excitation	400
Forced excitation	400-560
Constant excitation	560
Excitation reduction	560-460

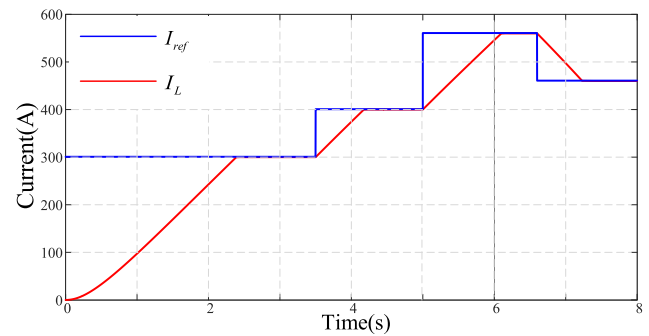


FIGURE 7. Simulation waveform of exciting current.

When the constant excitation is switched to the forced excitation, the exciting current will not immediately switch to being powered by the high voltage power supply. This state will remain until the diode  $D_3$  is turned off under the reverse voltage from the high voltage capacitor  $C_1$ . The current circuit at this time is shown in Fig. 5.

When the de-excitation mode works, the current circuit is shown in Fig. 6. In this mode, the switches  $G_1$  and  $G_2$  are turned off, and the reverse voltage from  $C_1$  is directly applied to the excitation winding through the freewheel diode  $D_1$  and  $D_2$ , making the exciting current decline rapidly.

It can be seen from Fig. 3 to Fig. 6 that under different working modes, by controlling the switches, the current circuit of the topology is different, and the working power supply is also inconsistent, so that the forced excitation and constant excitation of dual power supply can work separately.

### III. SIMULATION ANALYSIS OF EXCITATION SYSTEM

Based on the principle analysis, the viability of the proposed topology is further verified by simulation. The simulation parameters are shown in Table 1.

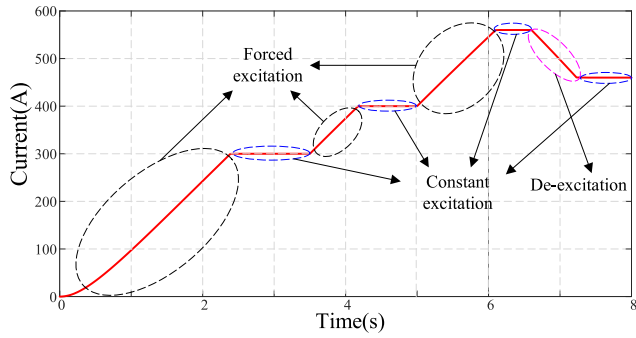


FIGURE 8. Schematic diagram of working mode.

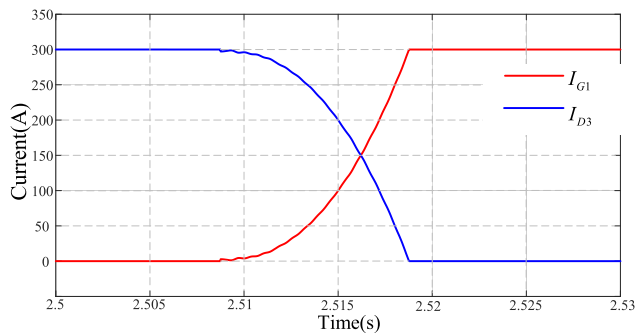


FIGURE 9. Current variation from constant excitation mode to forced excitation mode.

The working values of different exciting current for the HTS synchronous condenser are listed in Table 2. And the initial value of the exciting current is 0A.

Fig. 7 displays the simulation waveform of exciting current, where  $I_{ref}$  is the given value of exciting current and  $I_L$  is the actual value of exciting current. It can be seen that the actual value can well follow the given value of current.

Fig. 8 shows the working mode of the exciting current corresponding to each time period. It's shown that the exciting current can be stably held at the desired value in the constant excitation, and it also can be increased by 300A within 3 seconds in the forced excitation.

Fig. 9 displays the current variation of the excitation system when switching from constant excitation mode to forced excitation mode.

Since it is difficult to find the inductive load matching the actual HTS excitation winding, this experiment only uses 25mH superconducting coil as the load for experimental verification. Fig. 11 is the experimental field of the superconducting experiment.

From Fig. 7 to Fig. 9, it can be seen that the excitation system proposed in this paper operates well. And the simulation results are consistent with the desired value. The effectiveness of two power supplies for different working modes is verified.

#### IV. EXPERIMENT OF EXCITATION SYSTEM

According to the parameters of 10Mvar HTS synchronous condenser, a set of 400kW excitation system is designed. As shown in Fig. 10, the two cabinets are forced

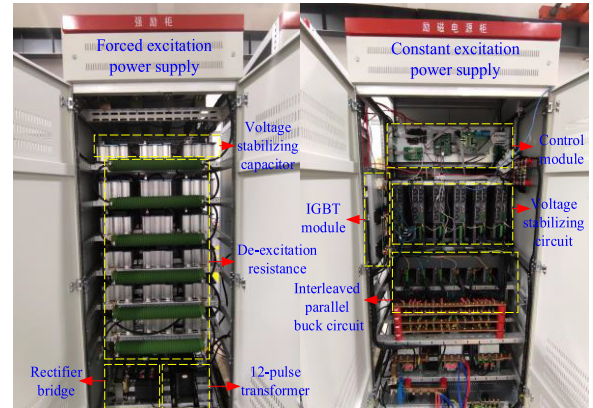


FIGURE 10. Installation of excitation power supply.

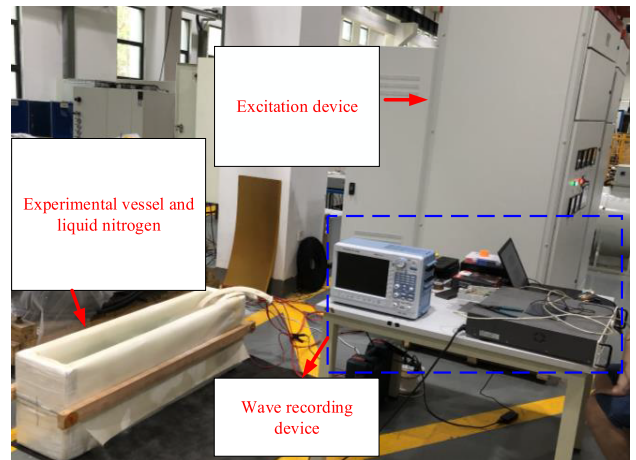


FIGURE 11. Superconducting experimental field.

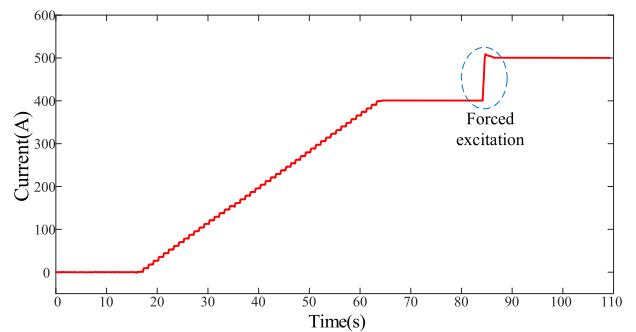


FIGURE 12. Experimental process waveform.

excitation power supply and constant excitation power supply respectively.

Firstly, the exciting current is slowly increased from 0A to 400A by low-voltage power supply, and then maintained at 400A for a certain time, so as to verify the stability of constant excitation control. Then, the exciting current is rapidly increased from 400A to 500A by the high-voltage forced excitation power supply, so as to verify whether the high-voltage forced excitation power supply works normally. Fig. 12 is the actual current waveform of the whole

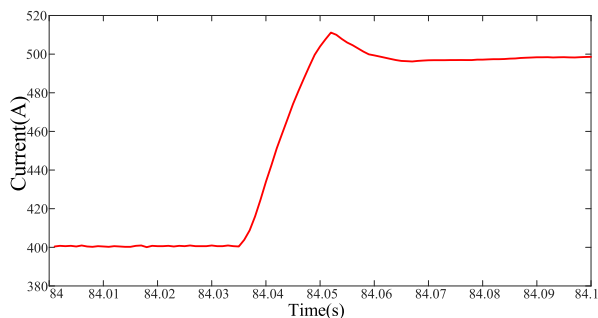


FIGURE 13. Forced excitation process waveform.

experimental process. Fig. 13 shows the specific waveform when the exciting current rise from 400A to 500A by the forced excitation power supply.

It can be seen from Fig. 12 and Fig. 13 that the actual process of forced excitation has a certain overshoot. Since the equivalent inductance of the excitation winding used in the experiment is only 25mH, it is far less than the actual inductance, and this problem cannot be avoided. For the actual 5.86H superconducting rotor, the overshoot will be greatly reduced.

## V. CONCLUSION

A set of high-low voltage switching excitation system for 10Mvar HTS synchronous condenser is proposed in this paper:

- 1) Different from conventional excitation power supply, this excitation system can separate forced excitation and constant excitation modes, thus it can respectively provide a steady output exciting current and adjust the current in wide range within a short time.
- 2) This paper designs each module of the excitation power supply, and a interleaved parallel buck circuit is applied to the constant excitation mode. The simulation analysis also verify the viability of the design.
- 3) Based on the theoretical analysis, a 400kW device is designed and completed. The superconducting experiment is carried out for this device, and the experimental results show the feasibility and reliability of the excitation system designed in this paper.

The design of this excitation system avoiding a series of problems such as low power factor and large harmonic at the AC side caused by the use of single power supply control, which has a certain application prospect and application advantages.

## REFERENCES

- [1] P. Song, Z. Shi, Q. Wu, Y. Yang, L. Zhang, B. Wu, M. Song, and T. Qu, "General design of a 300-kvar HTS synchronous condenser prototype," *IEEE Trans. Appl. Supercond.*, vol. 30, no. 4, pp. 1–5, Jun. 2020, doi: [10.1109/TASC.2020.2989788](https://doi.org/10.1109/TASC.2020.2989788).
- [2] W. Yating, Z. Yichi, Z. Qinyong, L. Zhiqiang, and J. Yilang, "Study on application of new generation large capacity synchronous condenser in power grid," *Power Syst. Technol.*, vol. 41, no. 1, pp. 22–28, 2017.

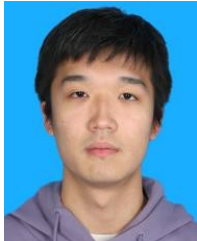
- [3] S. S. Kalsi, D. Madura, G. Snitchler, M. Ross, J. Voccio, and M. Ingram, "Discussion of test results of a superconductor synchronous condenser on a utility grid," *IEEE Trans. Appl. Supercond.*, vol. 17, no. 2, pp. 2026–2029, Jun. 2007, doi: [10.1109/TASC.2007.899206](https://doi.org/10.1109/TASC.2007.899206).
- [4] T. D. Le, J. H. Kim, D. J. Kim, C. J. Boo, Y. S. Jo, Y. S. Yoon, K. Y. Yoon, Y. H. Choi, H. Lee, and H. M. Kim, "Design of indirect closed-cycle cooling scheme coupled with a cryocooler for a 3-MW-class high-temperature superconducting synchronous motor," *IEEE Trans. Appl. Supercond.*, vol. 26, no. 4, pp. 1–4, Jun. 2016, doi: [10.1109/TASC.2016.2544812](https://doi.org/10.1109/TASC.2016.2544812).
- [5] A. Malozemoff, B. Kehrl, J. Diazdeleon, and S. Kalsi, "Superconducting technologies for a controllable and reliable high capacity grid," in *Proc. IEEE Power Eng. Soc. Gen. Meeting*, Denver, CO, USA, Jun. 2004, p. 2276.
- [6] S. S. Kalsi, D. Madura, and M. Ingram, "Superconductor synchronous condenser for reactive power support in an electric grid," *IEEE Trans. Appl. Supercond.*, vol. 15, no. 2, pp. 2146–2149, Jun. 2005, doi: [10.1109/TASC.2005.849481](https://doi.org/10.1109/TASC.2005.849481).
- [7] M. Frank, P. van Hasselt, P. Kummeth, P. Masek, W. Nick, H. Rothfischer, H. Schmidt, B. Wacker, H.-W. Neumuller, G. Nerowski, J. Frauenhofer, R. Hartig, and W. Rzaeki, "High-temperature superconducting rotating machines for ship applications," *IEEE Trans. Appl. Supercond.*, vol. 16, no. 2, pp. 1465–1468, Jun. 2006, doi: [10.1109/TASC.2005.849481](https://doi.org/10.1109/TASC.2005.849481).
- [8] Q. Wu, P. Song, Y. Yan, Z. Shi, M. Song, and T. Qu, "Design and testing of a gas-helium conduction cooled REBCO magnet for a 300 kvar HTS synchronous condenser prototype," *IEEE Trans. Appl. Supercond.*, vol. 30, no. 4, pp. 1–5, Jun. 2020, doi: [10.1109/TASC.2020.2974443](https://doi.org/10.1109/TASC.2020.2974443).
- [9] Z. Shi et al., "Electromagnetic design of 10 MVAR superconducting synchronous condenser," *Southern Power Syst. Technol.*, vol. 15, no. 1, pp. 76–81, 2021.
- [10] Q. Wu, P. Song, Z. Shi, L. Zhang, Y. Yan, Z. Yang, L. Shao, and T. Qu, "Development and testing of a 300-kvar HTS synchronous condenser prototype," *IEEE Trans. Appl. Supercond.*, vol. 31, no. 5, pp. 1–5, Aug. 2021, doi: [10.1109/TASC.2021.3061922](https://doi.org/10.1109/TASC.2021.3061922).
- [11] H. Wu, T. Mu, H. Ge, and Y. Xing, "Full-range soft-switching-isolated buck-boost converters with integrated interleaved boost converter and phase-shifted control," *IEEE Trans. Power Electron.*, vol. 31, no. 2, pp. 987–999, Feb. 2016, doi: [10.1109/TPEL.2015.2425956](https://doi.org/10.1109/TPEL.2015.2425956).
- [12] P. K. Jain and A. Kumar, "Interleaved DC to DC buck converter for low power application," in *Proc. Int. Conf. Energy, Power Environ., Towards Sustain. Growth (ICEPE)*, Jun. 2015, pp. 1–5.



**JINFENG WANG** is currently a Senior Engineer with the Electric Power Research Institute of Guangdong Power Grid Company Ltd., where he is engaged in power distribution technology research and standard formulation, including distribution network equipment operation analysis, power quality, and power supply reliability. He is also the Deputy Director of the Distribution Network Institute of the Electric Power Research Institute of Guangdong Power Grid Company Ltd., and the Master's Tutor with North China Electric Power University, where he has been engaged in research on power distribution technology for a long time. Facing the front-line needs of production and the industry's technological frontier, he has carried out major technical research and achievement cultivation and transformation in the areas of intelligent operation and maintenance of distribution networks and digital transformation, distribution network disaster prevention and reduction, and new power systems. He is a member of the Energy Industry Distribution Network System Standardization Committee and Guangdong Provincial Power Electronics System and Equipment Standardization Committee.



**TIANTIAN CAO** was born in Anqing, Anhui, China. She is currently pursuing the master's degree with Huazhong University of Science and Technology. Her research interest includes the power quality optimization of power systems.



**YUFENG DAI** was born in Hubei, China, in 1999. He received the B.S. degree in electrical engineering from China Three Gorges University, Yichang, China, in 2021. He is currently pursuing the M.S. degree in electrical engineering with Huazhong University of Science and Technology, Wuhan, China. His research interests include power quality harnessed synth ethically and grid-connected inverter control.



**SIQI XIE** was born in Chongqing, China, in 2000. He received the B.S. degree in electrical engineering from Tianjin University, Tianjin, China, in 2022. He is currently pursuing the M.S. degree in electrical engineering with Huazhong University of Science and Technology, Wuhan, China. His research interests include excitation regulators and control strategies for grid-connected inverters.



**ZHU LIU** received the bachelor's degree in electrical engineering and automation from Huazhong University of Science and Technology, in 2004, and the master's degree in electrical engineering from Xi'an Jiaotong University, in 2007. He is currently pursuing the Ph.D. degree with Huazhong University of Science and Technology.

He has been with Southern Power Grid, since 2007. He is the General Manager and a Senior Engineer with China Southern Power Grid Research Technology Company Ltd., where has been engaged in dispatching and operation, safety risk management, distribution network management, and new power system construction for a long time.



**DAYI LI** (Member, IEEE) received the B.S. degree from Tianjin Polytechnic University, Tianjin, China, in 1995, and the M.S. and Ph.D. degrees from Huazhong University of Science and Technology (HUST), Wuhan, China, in 2000 and 2005, respectively. From 1995 to 1997, he was an Electrical Engineer with Wuhan No.3 Cotton Mill Company, Wuhan. In 2000, he joined HUST as an Assistant Professor, where he is currently a Professor. From 2011 to 2012, he was a Visiting

Researcher with the Department of Electronic and Electrical Engineering, The University of Sheffield, Sheffield, U.K. His research interests include power quality controllers, transformers, and power electronics.

• • •